Relativistically Transparent Magnetic Filaments:

a path to megaTesla fields, direct electron acceleration, and efficient gamma radiation

Schematic of a magnetic filament

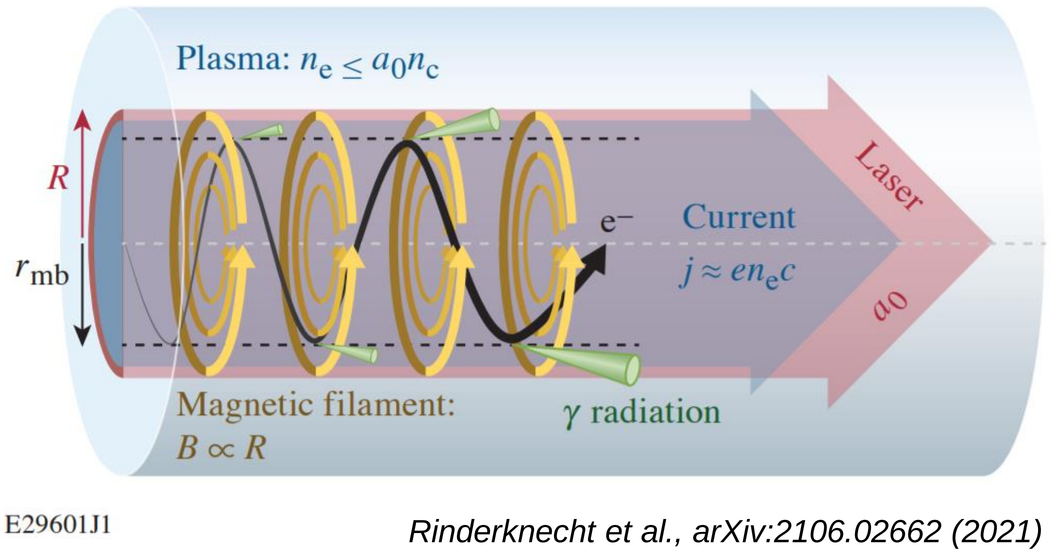

Rinderknecht et al., arXiv:2106.02662 (2021)

MeV photon radiation

(3-D PIC simulation, 5×10^{22} W/cm^2)

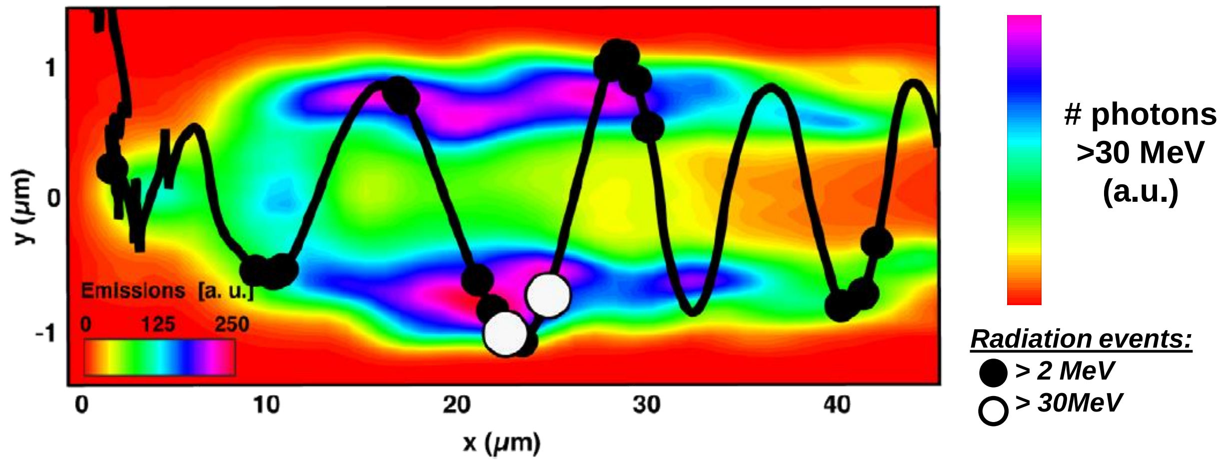

Stark et al., PRL 116, 185003 (2016)

Hans Rinderknecht
University of Rochester
Laboratory for Laser Energetics

4th Extremely High Intensity Laser Physics Conference
Wednesday, Sept 15, 2021

Magnetic filaments promise a repeatable and efficient laser-driven source of MT fields, relativistic electrons, and MeV photons

- **Intense lasers in relativistically transparent plasmas generate ultra-strong magnetic fields, trapping and accelerating electrons**
  - Relativistic electrons in ultra-strong B-fields efficiently radiate MeV-scale photons
- **Scaling laws were derived for magnetic filament radiation, and validated with 3-D PIC simulations**
  - Efficiency of >10% is predicted for intensity above 6×10^{21} W/cm^2
- **Experiments on the Texas Petawatt laser have been performed to test these predictions**
  - The predicted electron and photon signatures were observed in a subset of experiments

Collaborators

LLE/UR:
- Hans Rinderknecht
- Mingsheng Wei
- Gerrit Bruhaug
- Kathleen Weichmann
- John Palastro
- Jon Zuegel

UCSD:
- Alexey Arefiev
- Tao Wang

HZDR:
- Toma Toncian
- Alejandro Laso Garcia

ELI-NP:
- Domenico Doria
- Klaus Spohr

Texas Pettawatt (TPW)/UT Austin:
- Hernan J. Quevedo
- Todd Ditmire

General Atomics (GA):
- Jarrod Williams
- Alex Haid

Johns Hopkins University:
- Dan Stutman

Outline

Classically, lasers can only interact with plasmas below a *critical density* at which electron waves prevent the laser entering the plasma

$$\omega_{pe} = \sqrt{\frac{n_e e^2}{m_e \epsilon_0}}$$

Plasma dispersion, n_e = 5e22 cm^{-3}

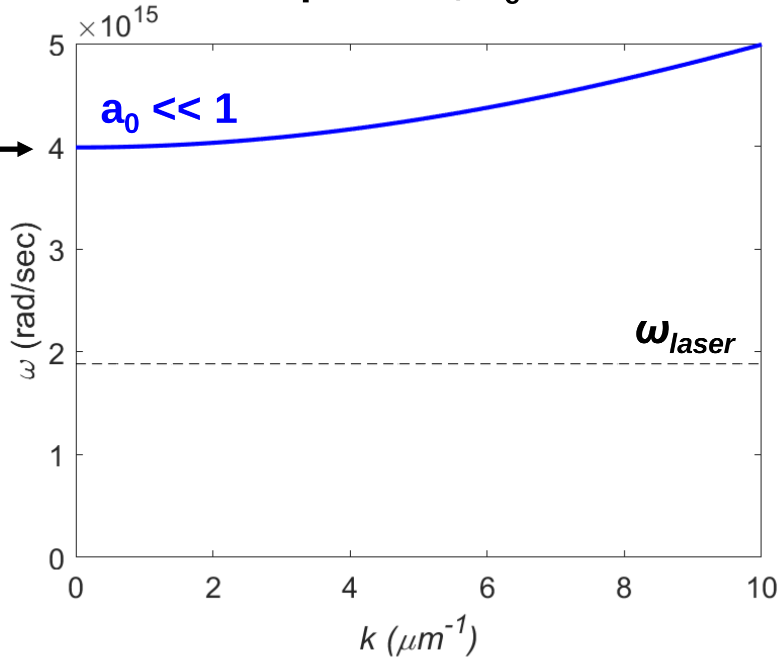

$$a_0 \equiv \frac{|e|E_0}{m_e \omega c}$$ *is the normalized laser amplitude: a_0 > 1 implies relativistic electrons*

$$\approx 0.86 \frac{\lambda}{\mu m} \sqrt{\frac{Intensity}{10^{18} W cm^{-2}}}$$

Non-relativistic motion

$$\varepsilon \propto p^2 \propto E_0^2$$

$$n_e < n_{crit} = \frac{\epsilon_0 m_e}{e^2} \omega_{laser}^2$$

Plasma oscillations at the laser frequency reflect the incident EM radiation

Laser-plasma interactions above the critical density are possible at high intensity (a_0 >> 1) due to *relativistic transparency*

$$\omega_{pe} = \sqrt{\frac{n_e e^2}{m_e \epsilon_0}}$$

Plasma dispersion, n_e = 5e22 cm^{-3}

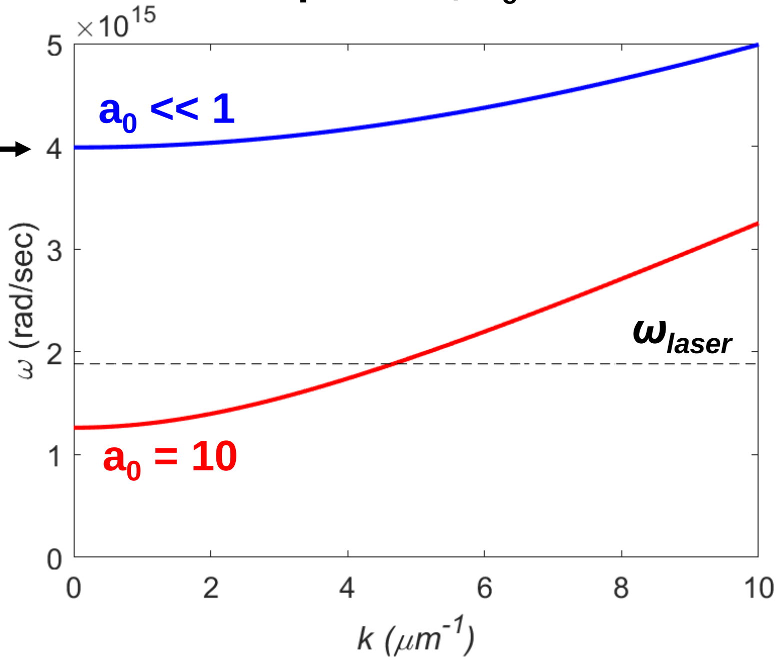

$$a_0 \equiv \frac{|e|E_0}{m_e \omega c}$$

$$\gamma = \sqrt{1 + a_0^2} \approx a_0$$

Non-relativistic motion

$$\varepsilon \propto p^2 \propto E_0^2$$

$$n_e < n_{crit} = \frac{\epsilon_0 m_e}{e^2}\omega_{laser}^2$$

Plasma oscillations at the laser frequency reflect the incident EM radiation

Ultra-relativistic motion

$$\varepsilon \propto p \propto E_0$$

$$n_e < a_0 n_{crit} = \frac{\epsilon_0 \gamma m_e}{e^2}\omega_{laser}^2$$

Relativistic plasma electrons have larger effective mass, increasing critical density

Relativistic transparency allows an intense laser pulse to propagate into an overdense plasma

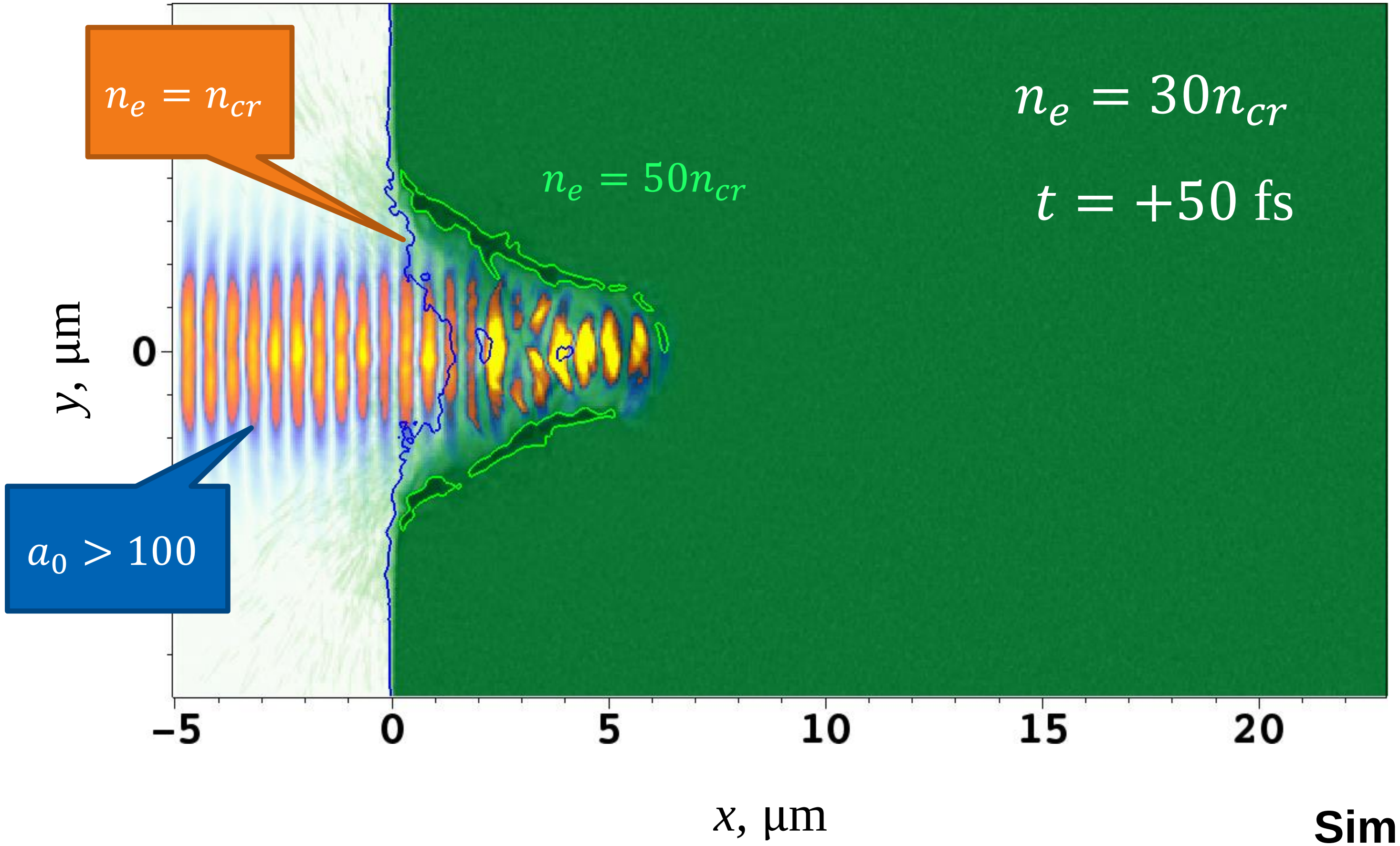

Simulations by A. Arefiev

However, relativistically transparent propagation is unstable

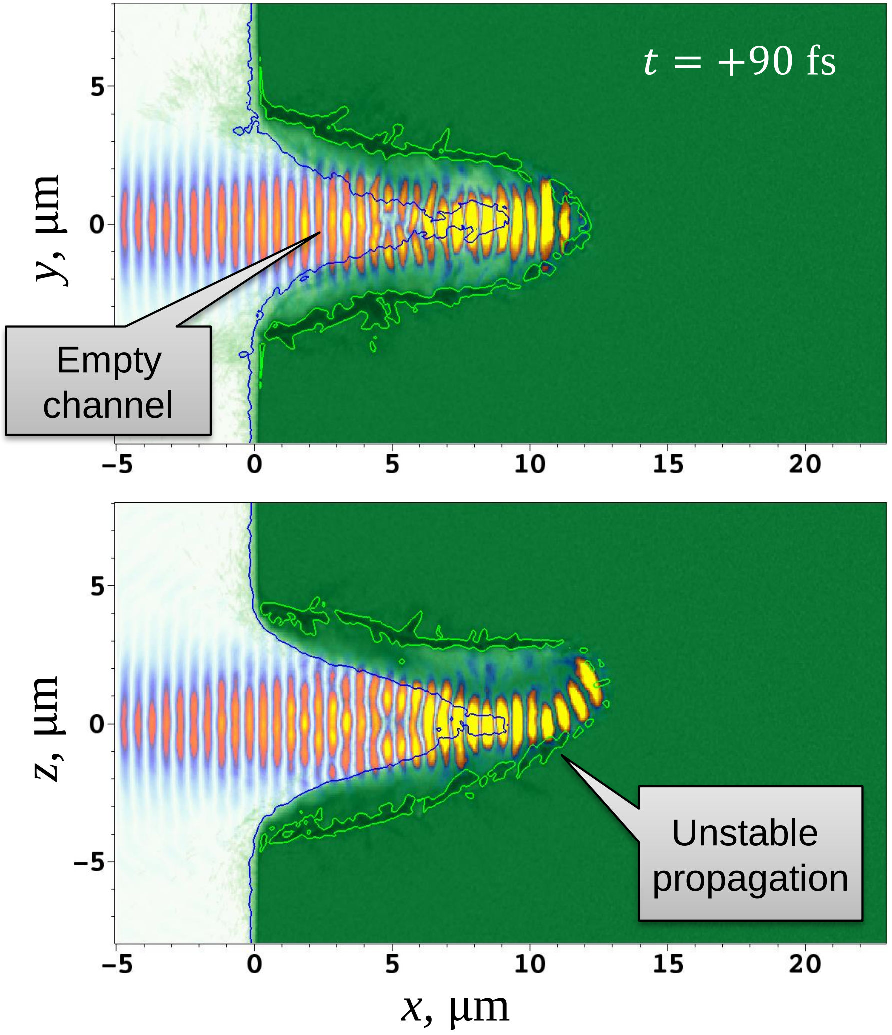

- The tightly focused laser pulse expels electrons laterally.
- The channel becomes empty, and laser pulse propagation deflects randomly.

This instability breaks the symmetry of the channel, impeding electron acceleration and subsequent high-energy photon production.

Simulations by A. Arefiev

Stability of interaction can be regained by using a structured target: a filled channel acts as a waveguide for the intense laser

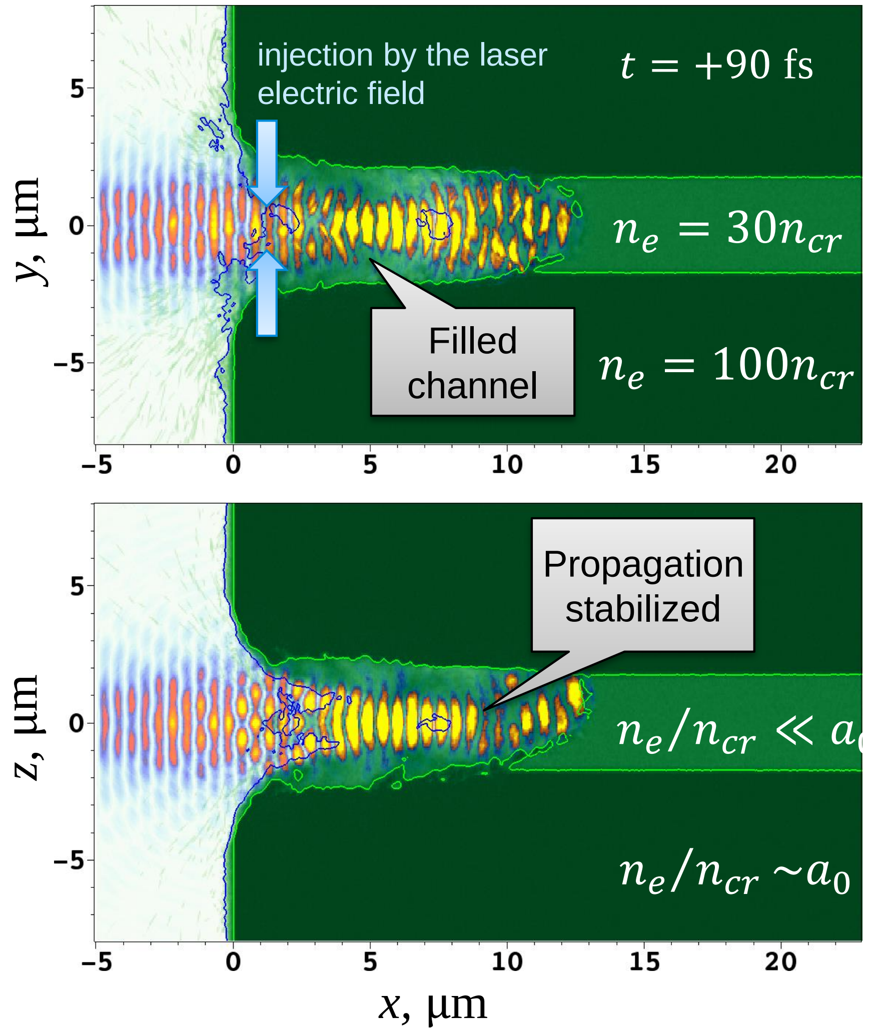

A structured target enables an effective long-term volumetric interaction with an overdense plasma.

Simulations by A. Arefiev

Outline

In relativistically transparent magnetic filaments, the ponderomotive force drives a relativistic current, producing a strong azimuthal magnetic field

3-D PIC simulations (a_0 = 50)[1]:

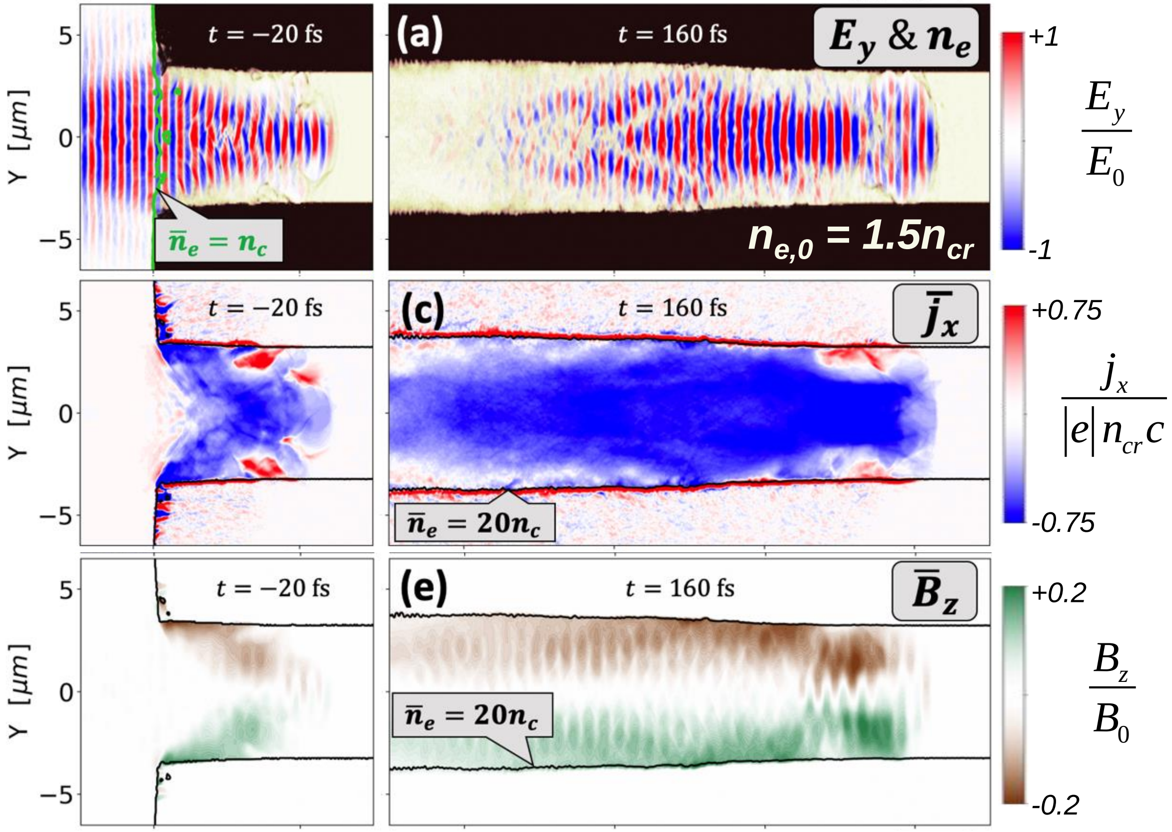

Magnetic field of current normalized to laser field:

$$\frac{B_j}{B_0} = \left(\frac{\mu_0 j r}{2}\right) \Big/ \left(\frac{2\pi a_0 mc}{e\lambda}\right)$$

$$= \pi \left(\frac{r}{\lambda}\right)\left(\frac{n_e \beta}{n_{cr} a_0}\right)$$

$$\equiv \pi r_\lambda S_\alpha$$

Quasi-static magnetic fields of the order of the oscillating laser field are produced and observed by electrons.

[1]Z. Gong, et al., Phys. Rev. E 102, 013206 (2020)

Electrons orbit within a magnetic boundary. Those in phase with the laser are accelerated, and radiate by deflecting in the strong magnetic field.

Magnetic field of current normalized to laser field:

$$\frac{B_j}{B_0} = \pi \left(\frac{r}{\lambda}\right)\left(\frac{n_e \beta}{n_{cr} a_0}\right) \equiv \pi r_\lambda S_\alpha$$

Magnetic boundary[1]:

$$\frac{r_{mb}}{\lambda} \approx \frac{1}{\pi}\sqrt{\frac{\gamma_i n_{cr}}{n_e}} \approx \frac{1}{\pi}\sqrt{\frac{f_i}{S_\alpha}}$$

$$\left(f_i \equiv \frac{\gamma_i}{a_0}\right)$$

The maximum magnetic field seen by electrons is limited by the *smaller* of focal radius and magnetic boundary.

Electron orbits & acceleration (a_0 = 50)[1]

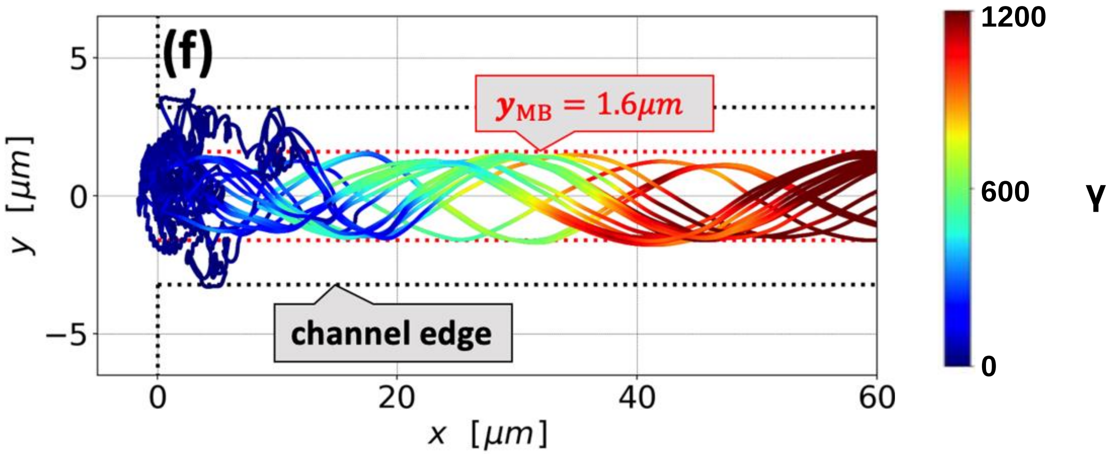

Photon radiation (a_0 = 190)[2]

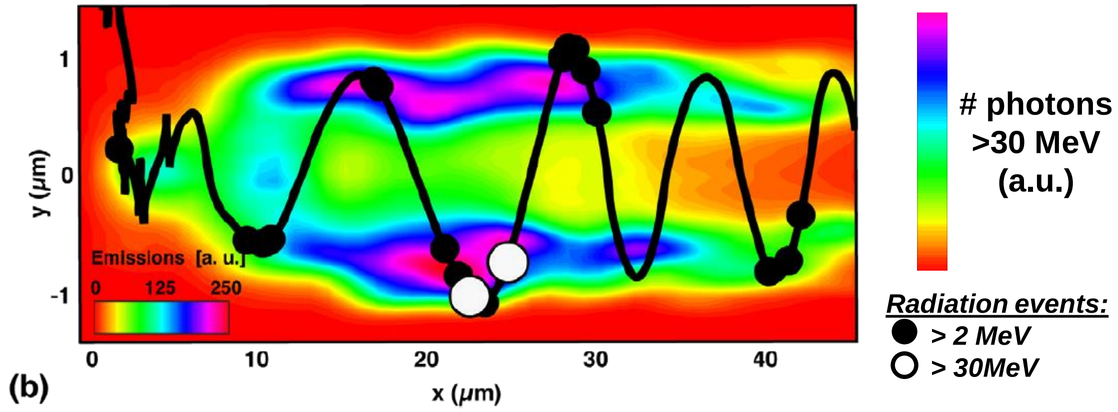

[1]Z. Gong, et al., Phys. Rev. E 102, 013206 (2020)
[2]D. J. Stark, et al., Phys. Rev. Lett. 116, 185003 (2016)

Using simple assumptions for the electron acceleration and orbits, we derive scaling laws for the radiation from magnetic filaments

1: Electrons are thermal

$$f_e(\epsilon_e, t) = \frac{N_e}{T_e}\exp\left[-\frac{\epsilon_e}{T_e}\right], \quad \text{where} \quad N_e = n_e\left(\pi R^2\right)(c\tau)$$

2: Electron acceleration is linear in time

$$T_e(t) = C_T a_0 \left(\frac{ct}{\lambda}\right) mc^2 \equiv C_T a_0 t_\nu mc^2$$

3: Radiation is synchrotron-like

$$\frac{dP}{d\epsilon_*} = f_r \frac{4}{9}\alpha_{fsc}\frac{mc^2}{\hbar}\left(\frac{B}{B_{cr}}\right)F\left[\frac{\epsilon_*}{\epsilon_c}\right], \quad \text{where} \quad \epsilon_c = \frac{3}{2}\chi\gamma mc^2, \quad F[x] \equiv \frac{9\sqrt{3}}{8\pi}x\int_x^\infty K_{5/3}(z)\,dz \quad \left[\int_0^\infty F(y)dy = 1\right]$$

4: The laser depletes by heating electrons

$$\frac{E_e}{E_{Laser}} \le 1 \quad \rightarrow \quad t_{\nu,\max} \le \frac{\sqrt{\pi}}{4(\ln 2)^{3/2}}\frac{1}{C_T S_\alpha}. \qquad \text{We define: } t_{\nu,cut} \equiv f_t t_{\nu,max} \approx 0.768\frac{f_t}{C_T S_\alpha}$$

These assumptions have four constants: f_i, f_t, f_r, C_T and four design parameters: a_0, S_α, R/λ, cτ/λ

H.G. Rinderknecht, et al., New Journal of Physics (accepted) doi: 10.1088/1367-2630/ac22e7

Scaling laws are calculated as moments of the radiated photon spectrum integrated over photon energy, electron energy, and time.

…if focal radius R < r_{mb}:

$$\frac{\langle \epsilon_* \rangle_{tot}}{m_e c^2} \approx 1.38\times10^{-6}\ f_t^{\,2} a_0^3 S_\alpha^{-1} R_\lambda \lambda_{\mu m}^{-1}$$

$$\frac{E_{\gamma,tot}}{m_e c^2} \approx 7.74\times10^{2}\ f_r f_t^{\,3} C_T^{\,-1} a_0^{\,5} R_\lambda^{\,4} \tau_\nu$$

$$N_{\gamma,tot} = 5.59\times10^{8}\ f_r f_t C_T^{-1} a_0^{\,2} S_\alpha R_\lambda^{\,3} \tau_\nu \lambda_{\mu m}$$

$$\eta_\gamma = 2.88\times10^{-7}\ f_r f_t^{\,3} C_T^{\,-1} a_0^{\,3} R_\lambda^{\,2} \lambda_{\mu m}^{-1}$$

…if focal radius R > r_{mb}:

$$\frac{\langle \epsilon_* \rangle_{tot}}{m_e c^2} \approx 4.40\times10^{-7} \sqrt{f_i}\, f_t^{\,2} a_0^3 S_\alpha^{-3/2} \lambda_{\mu m}^{-1}$$

$$\frac{E_{\gamma,tot}}{m_e c^2} \approx 7.84\times10^{1}\ f_i f_r f_t^{\,3} C_T^{\,-1} a_0^{\,5} S_\alpha^{\,-1} R_\lambda^{\,2} \tau_\nu$$

$$N_{\gamma,tot} = 1.78\times10^{8} \sqrt{f_i}\, f_r f_t C_T^{-1} a_0^{\,2} S_\alpha^{1/2} R_\lambda^{\,2} \tau_\nu \lambda_{\mu m}$$

$$\eta_\gamma = 2.92\times10^{-8}\ f_r f_t^{\,3} f_i C_T^{\,-1} a_0^{\,3} S_\alpha^{\,-1} \lambda_{\mu m}^{-1}$$

H.G. Rinderknecht, et al., New Journal of Physics (accepted) doi: 10.1088/1367-2630/ac22e7

To test these scaling laws, we compared them to a series of 3-D PIC simulations that varied the focal radius

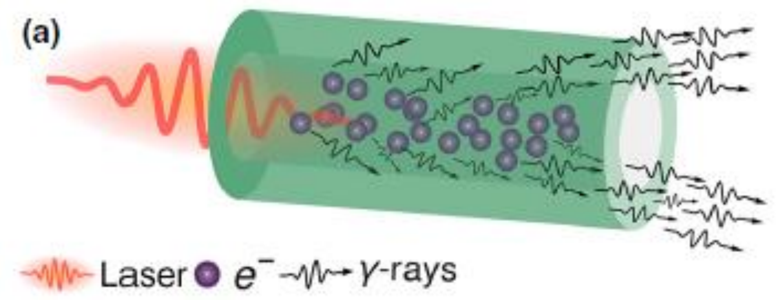

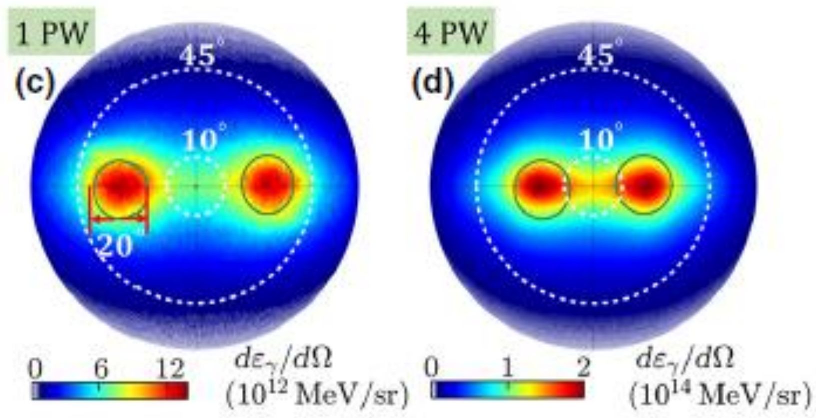

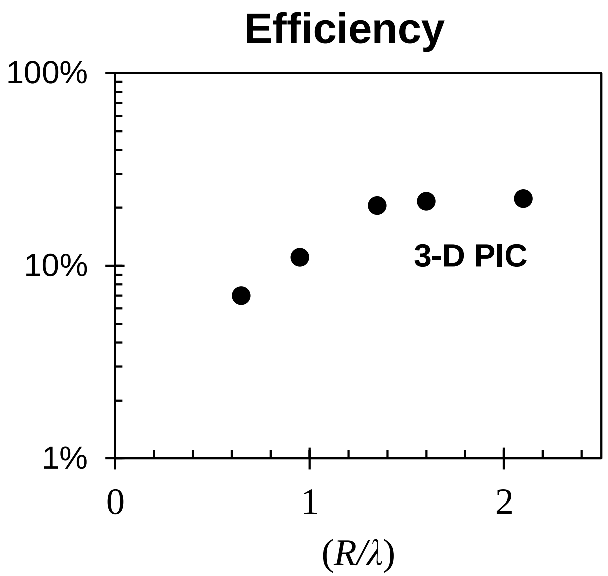

Parameters: a_0 = 190 (5×10^{22} W/cm^2)
S_α = 0.105 ($n_e = 20n_{cr}$)
R_λ = [0.65, 2.1]
τ_v = 10.5 (35 fs)

T. Wang, et al., Phys. Rev. Applied 13, 054024 (2020)

The scaling laws show good agreement with 3-D PIC simulations that varied the focal radius, with reasonable constants

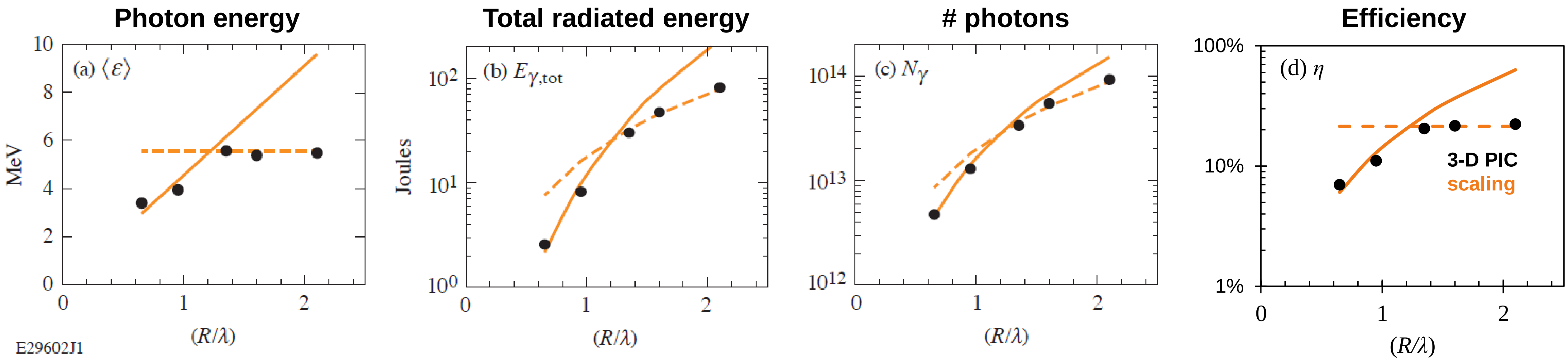

Parameters: a_0 = 190 (5×10^{22} W/cm^2)
S_α = 0.105 ($n_e = 20n_{cr}$)
R_λ = [0.65, 2.1]
τ_ν = 10.5 (35 fs)

Constants:

	f_i = 1.533,	initial electron momentum scalar,	$\gamma_i \equiv f_i a_0$
	f_t = 0.311,	cutoff time scalar,	$t_{\nu,cut} \equiv f_t t_{\nu,max}$
	f_r = 0.189,	radiation duty cycle,	$P \equiv f_r P_{synch}$

H.G. Rinderknecht, et al., New Journal of Physics (accepted) doi: 10.1088/1367-2630/ac22e7

Outline

Initial experiments to study relativistically transparent magnetic filaments were performed at the Texas Petawatt Laser (TPW)

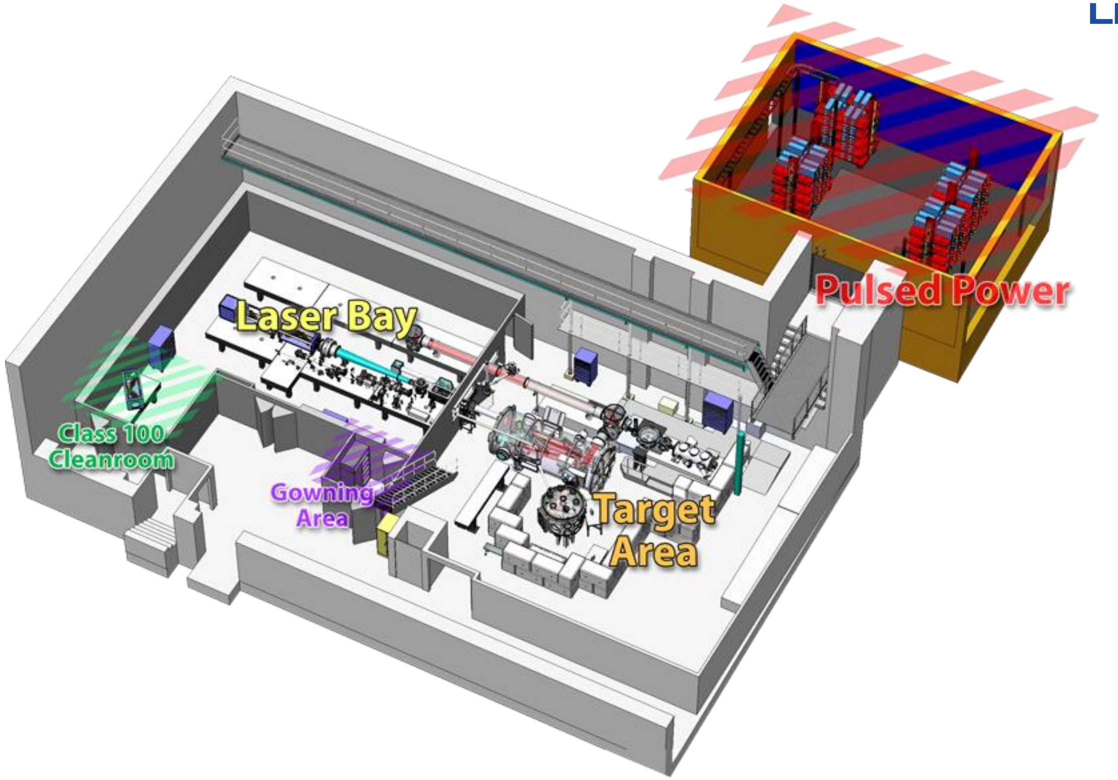

- Wavelength: 800 nm
- Energy: 98.8 ± 6.0 Joules
- Duration: 140 fs
- Power: 694 ± 38 TW

- Intensity: [1.09 ± 0.07]×10^{21} W/cm^2 (a_0 = 29.9 ± 1.0)
- Radius: 2.6 ± 0.12 μm (at 50% peak intensity)
- Pointing: 8-μrad rms
  → 5-μm rms on target

Microchannel targets filled with low-density foam (n_e = 5 or 10 n_{cr}) were developed for this campaign

Channels were laser-drilled in Kapton (6-μm diameter, 15-μm separation) and filled with low-density CH foam (15 or 30 mg/cm^3):

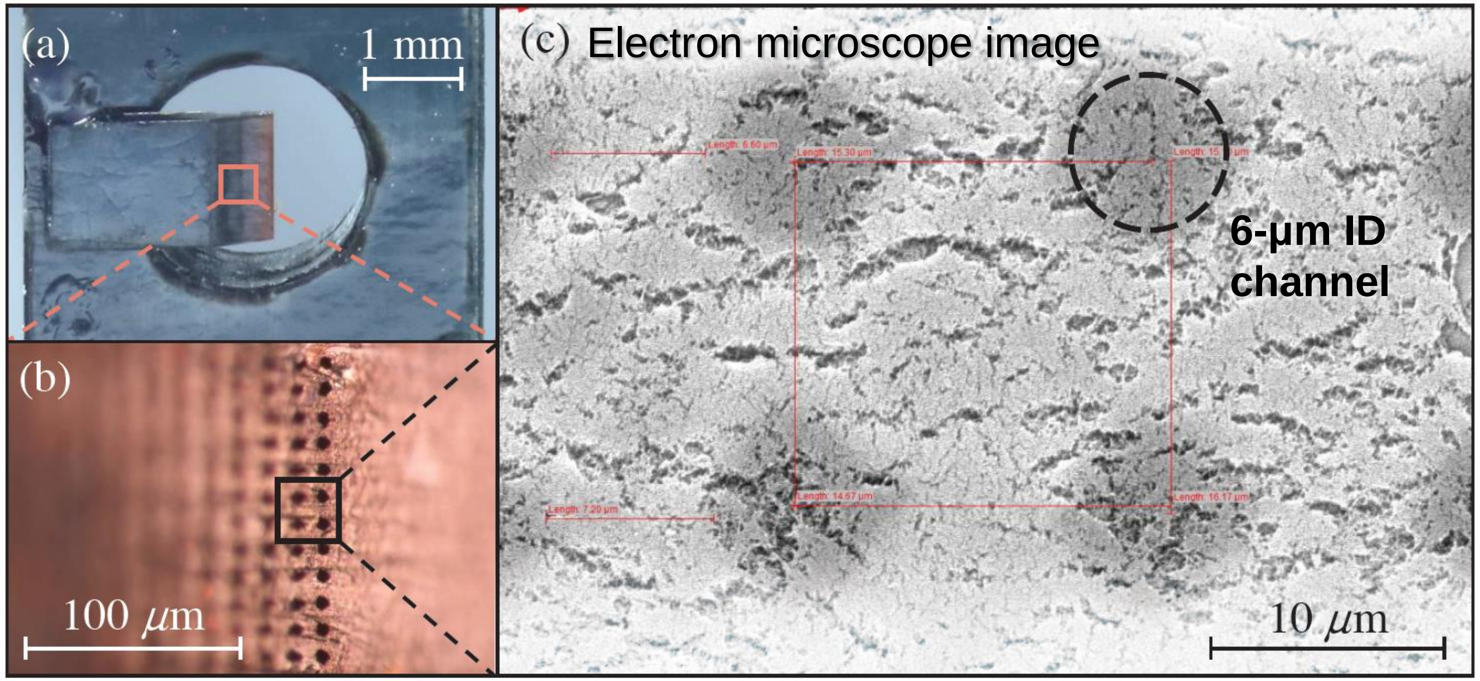

E29603J1

11 shots were performed with good laser-target alignment:

- **[×5] 6-μm ID, 5-n_{cr} fill**
- **[×3] 6-μm ID, 10-n_{cr} fill**
- **[×1] 6-μm ID, unfilled**
- **[×2] Planar 10-n_{cr} slab**

Given the pointing stability (5-μm rms), we did not expect to have channel interactions on every shot.

Primary diagnostics were an electron spectrometer (EPPS) and a gamma calorimeter (GCAL) in the expected radiation direction

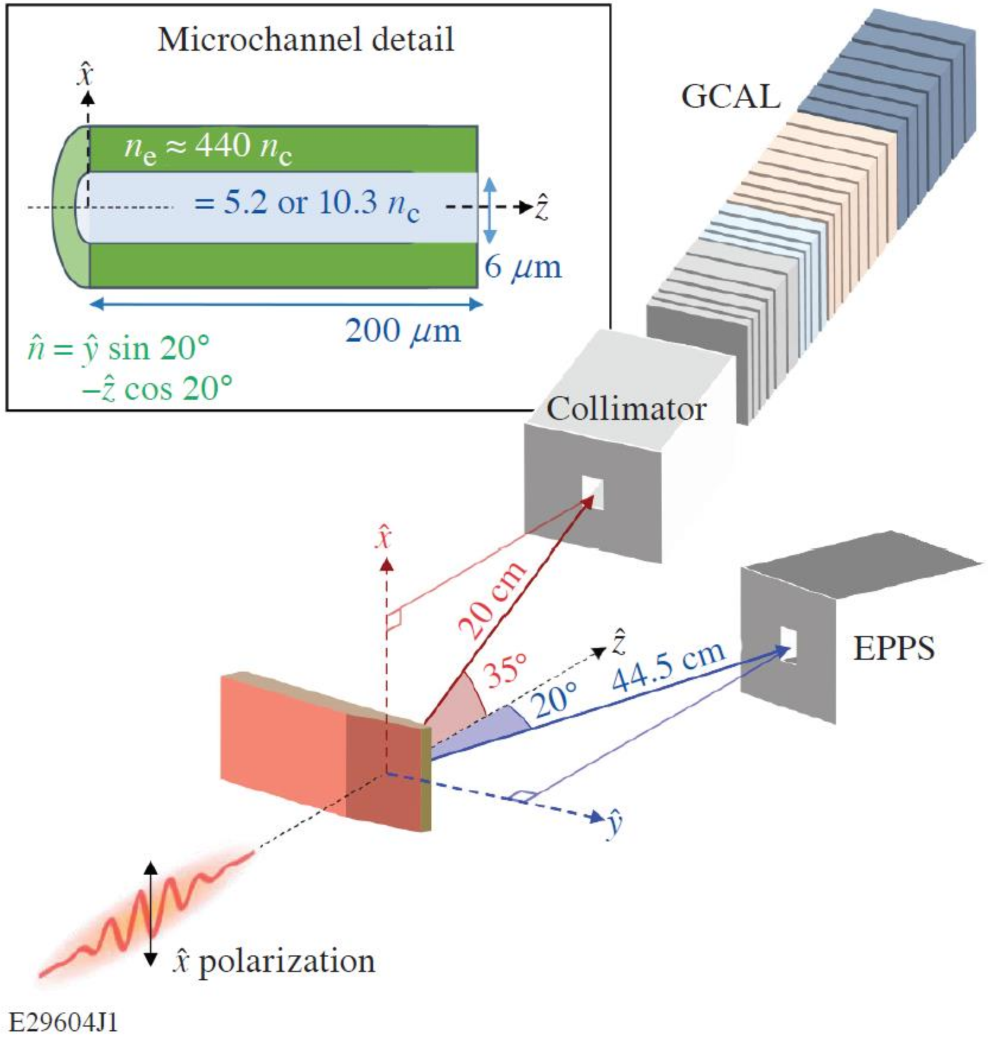

Simulated x-ray profiles (> 10 keV)

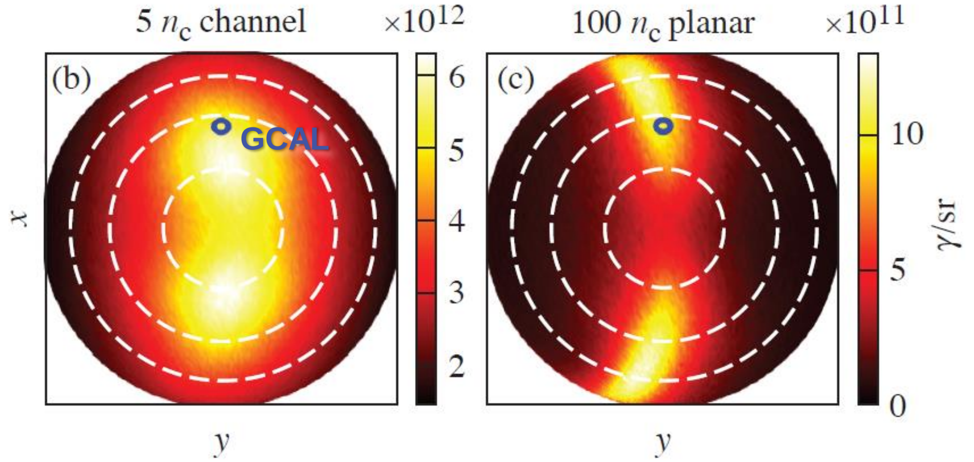

A factor of 5 difference in photon brightness is predicted between microchannel and 'solid' targets.

The 'hot' electron temperature was elevated on 2 of 8 microchannel shots

Electron temperatures

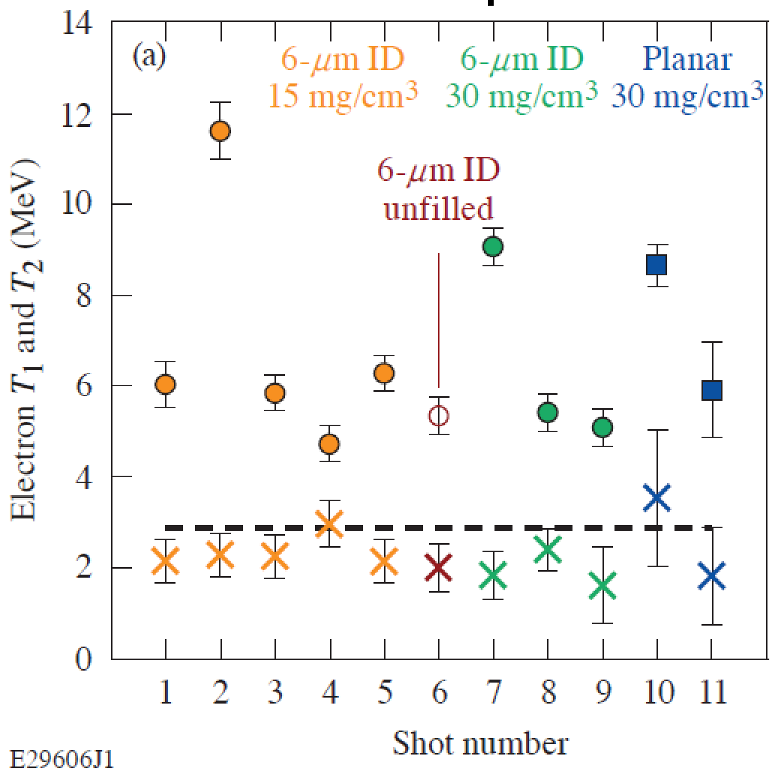

Example electron spectra

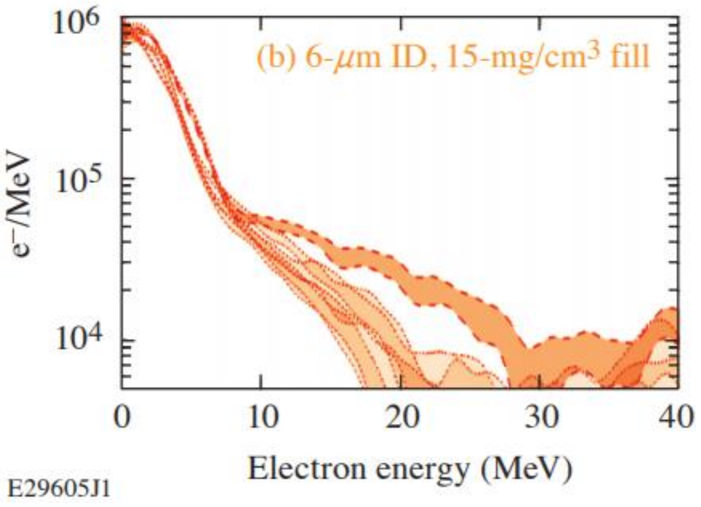

H.G. Rinderknecht, et al., New Journal of Physics (accepted) doi: 10.1088/1367-2630/ac22e7

The 'hot' electron temperature was elevated on 2 of 8 microchannel shots, consistent with the predicted magnetic filament behavior

Electron temperatures

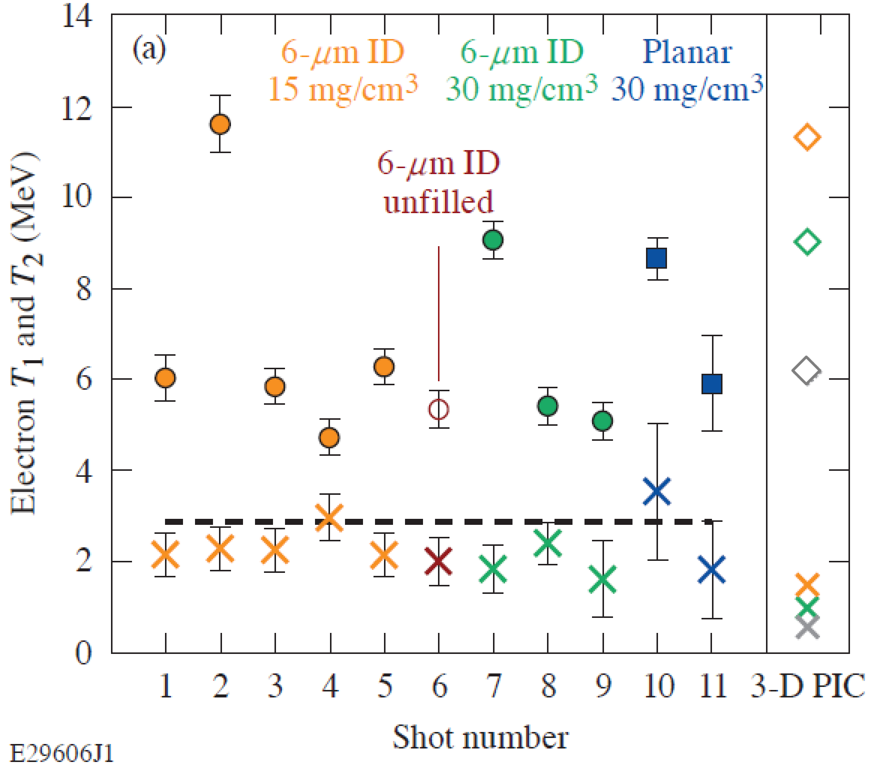

3-D PIC simulations:

15 mg/cm³ channel fill

30 mg/cm³ channel fill

"solid" (~0.6 g/cm³)

H.G. Rinderknecht, et al., New Journal of Physics (accepted) doi: 10.1088/1367-2630/ac22e7

The 'hot' electron temperature was elevated on 2 of 8 microchannel shots, consistent with the predicted magnetic filament behavior

Electron temperatures

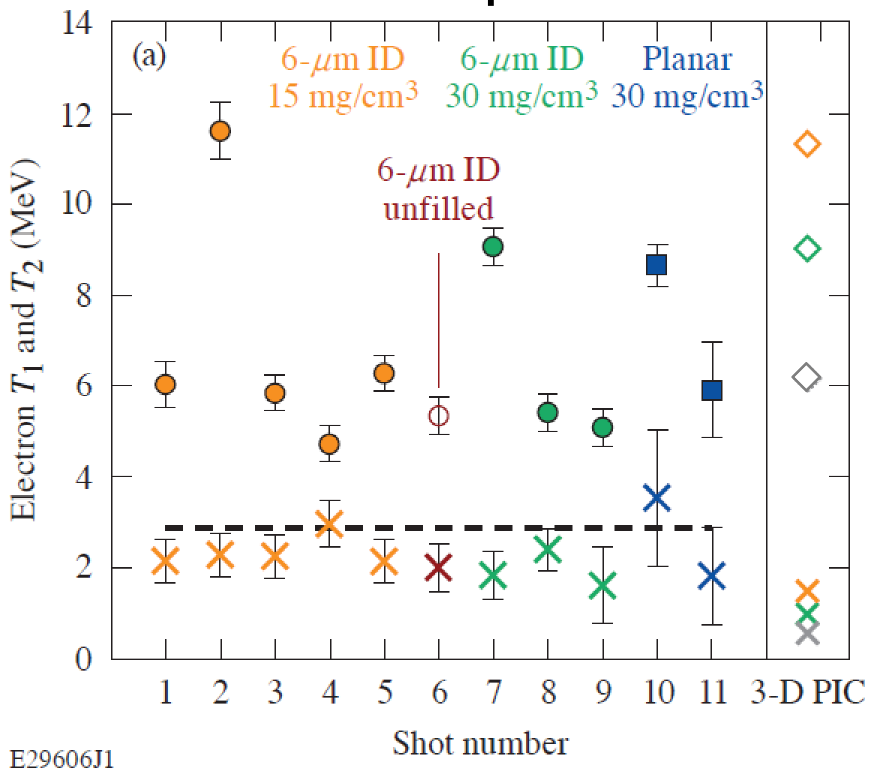

Given the pointing stability and channel size, the probability of observing N interactions is:

N	Probability
0	0.21
1	0.36
2	**0.27**
3	0.12
4	0.03
5+	< 0.01

We conclude that the predicted electron acceleration was observed in a subset of these experiments.

H.G. Rinderknecht, et al., New Journal of Physics (accepted) doi: 10.1088/1367-2630/ac22e7

The ‘hot’ electron temperature was elevated on 2 of 8 microchannel shots, consistent with the predicted magnetic filament behavior

UR LLE

Electron temperatures

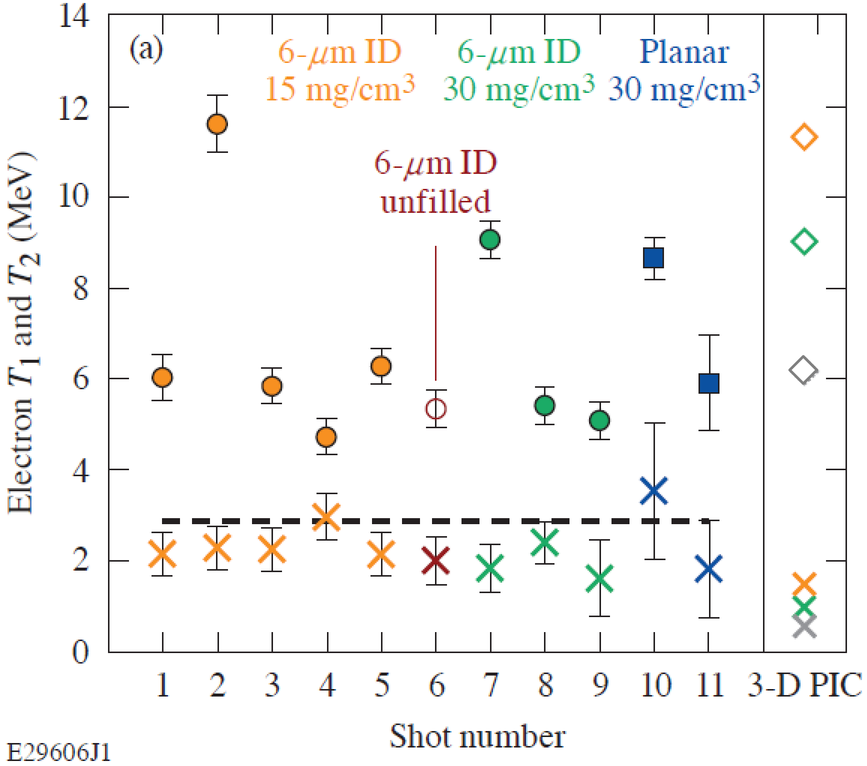

Electron T_{hot} vs # photons

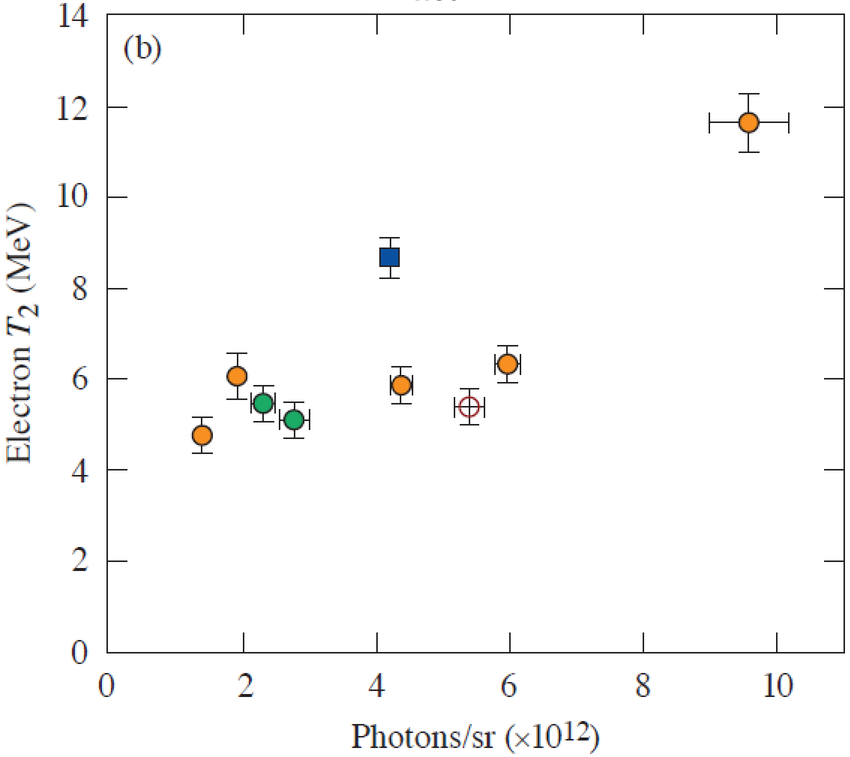

The number of photons > 10 keV also scaled with hot electron temperature as expected.

H.G. Rinderknecht, et al., New Journal of Physics (accepted) doi: 10.1088/1367-2630/ac22e7

Outline

For future experiments, closely packed channel arrays have been developed to improve repeatability and control over channel properties

Microchannel arrays in development

Top view:

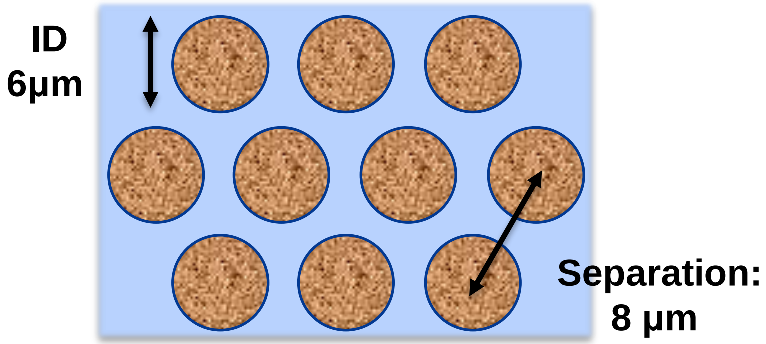

- Hexagonal close-packed array (20 by 20)
- Channel length: 100 μm minimum
- Foam density: 1—5 n_{crit} (ρ ~ 3—15 mg/cm^3)

Photo of array produced by 2-photon polymerization:

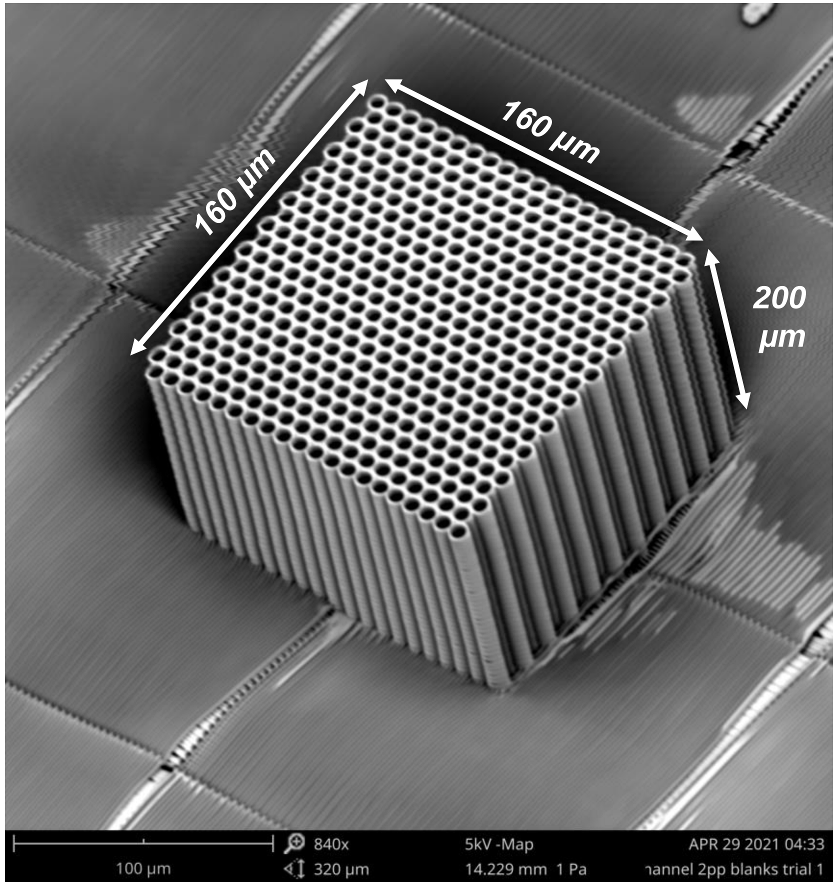

A. Haid, GA

For future experiments, a compound parabolic concentrator (CPC) design may enable robust laser coupling to a single channel

Simulation of a CPC target for NIF-ARC

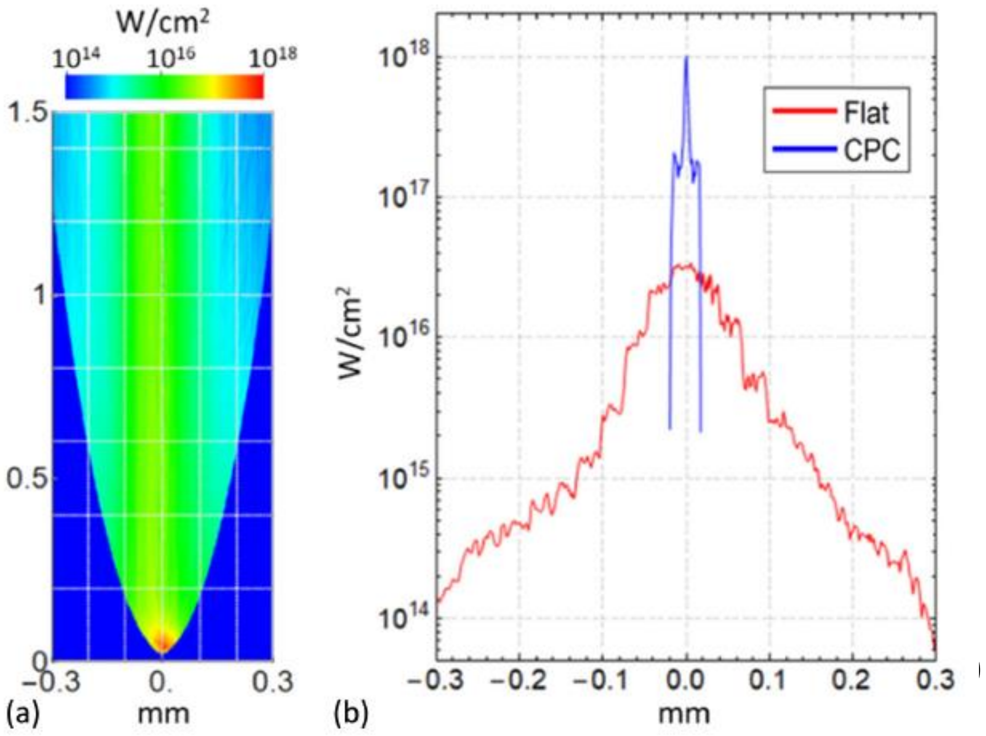

A. G. MacPhee, et al., *Optica* 7, 129 (2020).

CPC microchannel concept (A. Haid, GA)

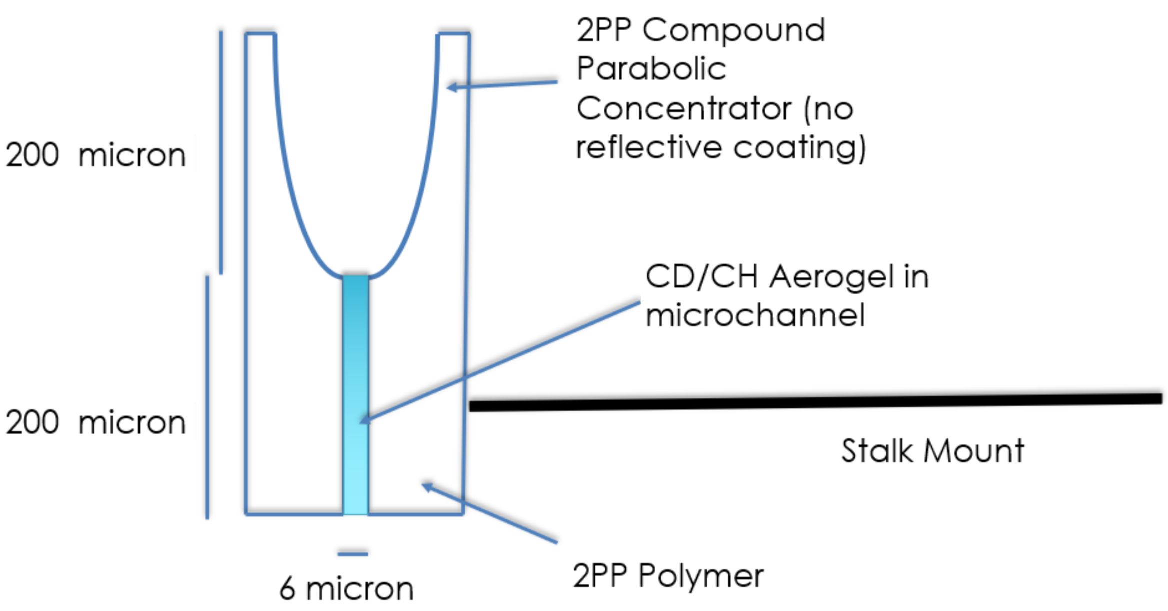

With 10-PW lasers now becoming available, magnetic filaments promise exciting opportunities for high-flux gamma-ray sources

UR LLE

Laser	ELI-NP†		ELI-Beamlines L4‡	
λ	0.8 μm		1.057 μm	
τ	23 fs		150 fs	
Peak power	10 PW		10 PW	
Intensity (a_0)	5×10^{22} W/cm^2 (153)		5×10^{22} W/cm^2 (202)	
Design choice:	**S_α = 0.01**	**S_α = 0.05**	**S_α = 0.01**	**S_α = 0.05**
Photon energy $\langle\varepsilon_*\rangle$	**68 MeV**	9.2 MeV	**96 MeV**	19 MeV
Total energy $E_{\gamma,tot}$	111 J	51 J	797 J	727 J
# photons N_γ	1.0×10^{13}	**3.5×10^{13}**	5.2×10^{13}	**2.5×10^{14}**
Efficiency η	48%*	22%*	53%*	48%*

By varying the channel design, the photon spectrum and flux may be optimized.

† D. Ursescu, et al., Romanian Reports in Physics 68, S11 (2016)
‡ S. Weber, et al., Matter and Radiation at Extremes 2, 149 (2017)

*model limited by radiation depletion

With 10-PW lasers now becoming available, magnetic filaments promise exciting opportunities for ultraintense HED experiments

- **Breit-Wheeler pair production**

Y. He, et al., Commun. Physics 4, 139 (2021)

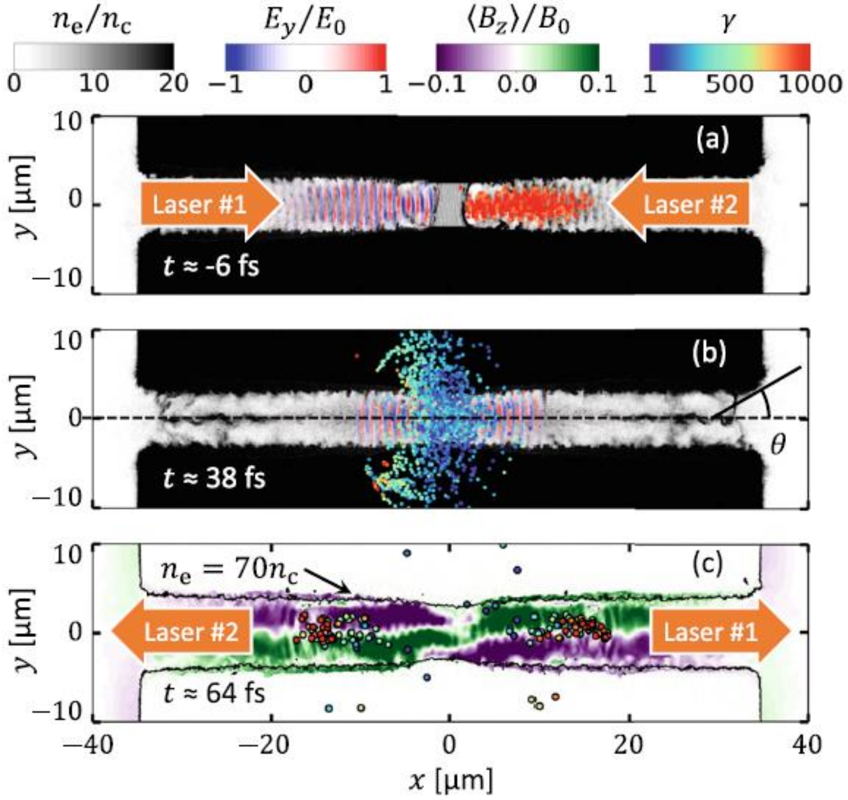

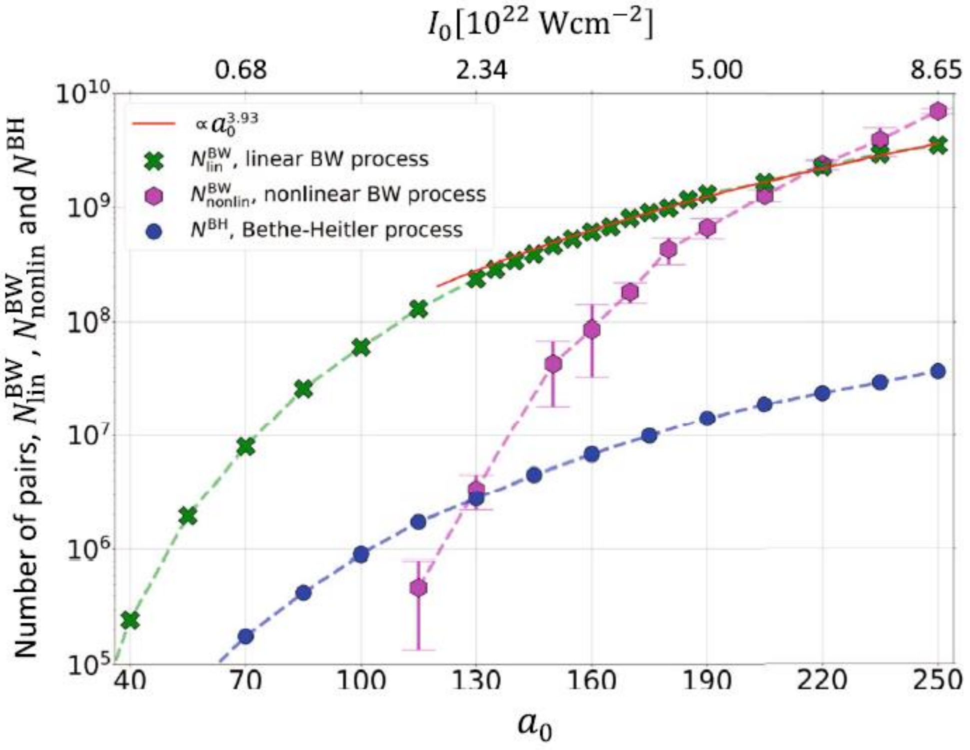

With 10-PW lasers now becoming available, magnetic filaments promise exciting opportunities for ultraintense HED experiments

- **Breit-Wheeler pair production**

Y. He, et al., Commun. Physics 4, 139 (2021)

- **MegaTesla fields in plasmas**

T. Wang, et al., Phys. Plasmas 26, 013105 (2019)

Proposed Faraday rotation measurement at EuXFEL

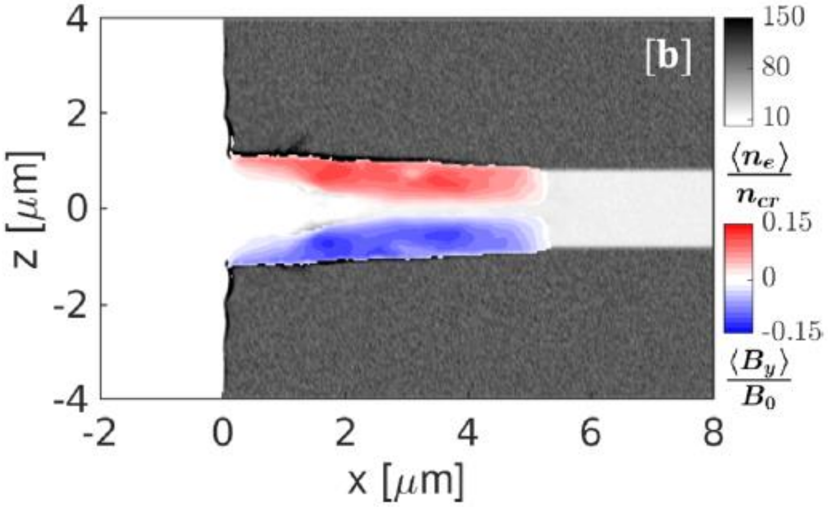

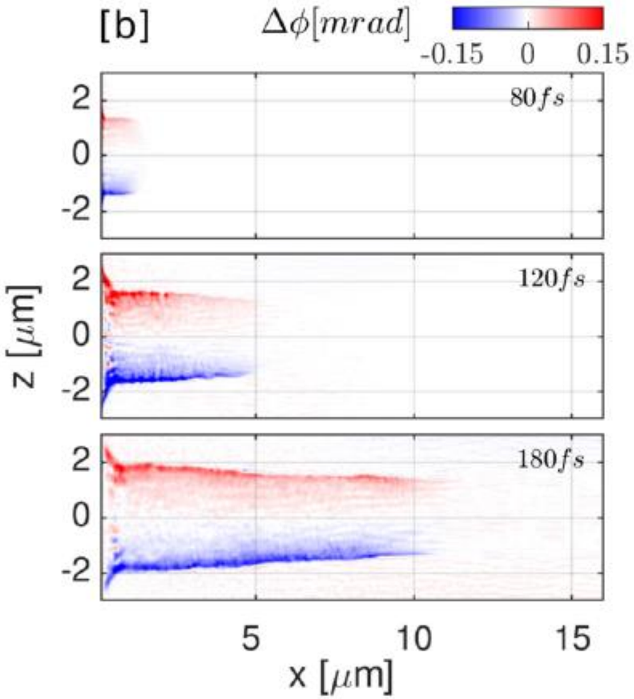

With 10-PW lasers now becoming available, magnetic filaments promise exciting opportunities for ultraintense HED experiments

- **Breit-Wheeler pair production**

Y. He, et al., Commun. Physics 4, 139 (2021)

- **MegaTesla fields in plasmas**

T. Wang, et al., Phys. Plasmas 26, 013105 (2019)

- **Collective dynamics with radiation reaction**

Z. Gong, et al., Sci. Reports 9, 17181 (2019)

Radiation friction changes electron orbits: this can prevent dephasing and enables much higher electron energies

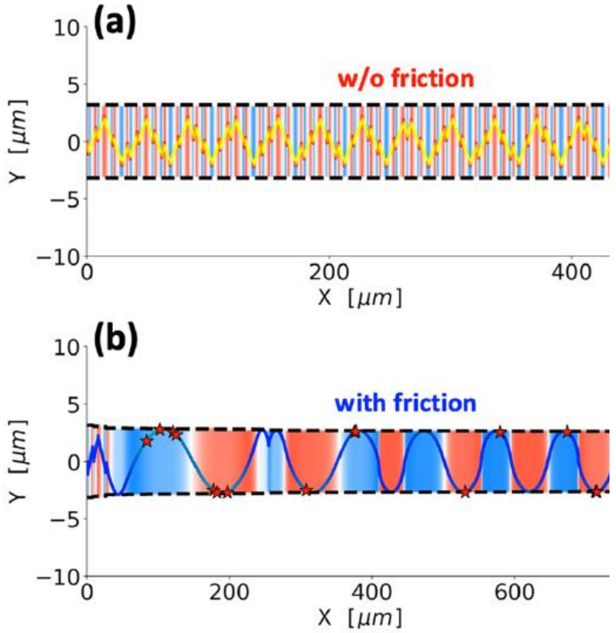

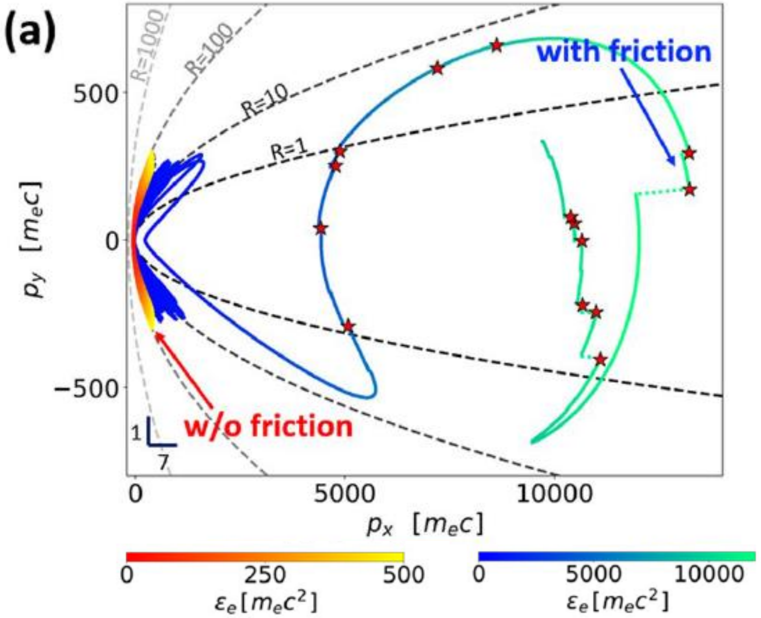

With 10-PW lasers now becoming available, magnetic filaments promise exciting opportunities for ultraintense HED experiments

- **Breit-Wheeler pair production**

Y. He, et al., Commun. Physics 4, 139 (2021)

- **MegaTesla fields in plasmas**

T. Wang, et al., Phys. Plasmas 26, 013105 (2019)

- **Collective dynamics with radiation reaction**

Z. Gong, et al., Sci. Reports 9, 17181 (2019)

- **Photofission for spent nuclear fuel processing**

T. Tajima, et al., Uspekhi Climate Change Forum (2021)

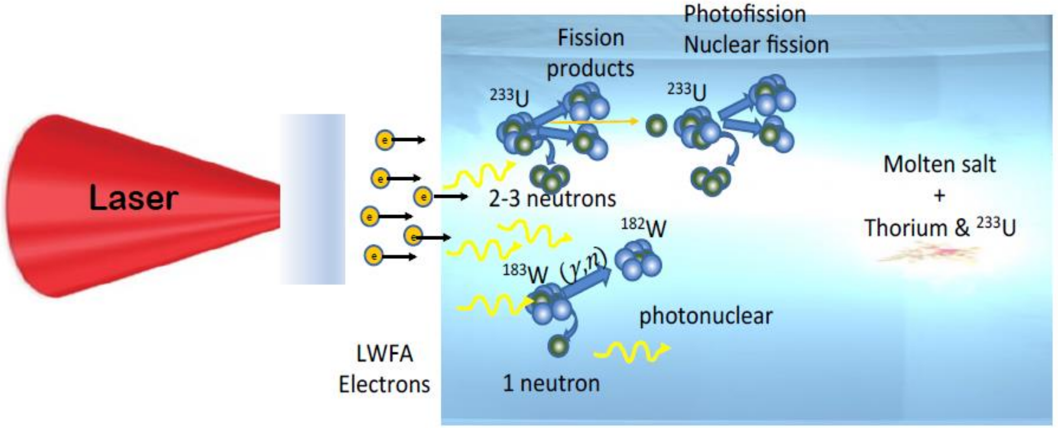

Toxicity vs time for spent nuclear fuel

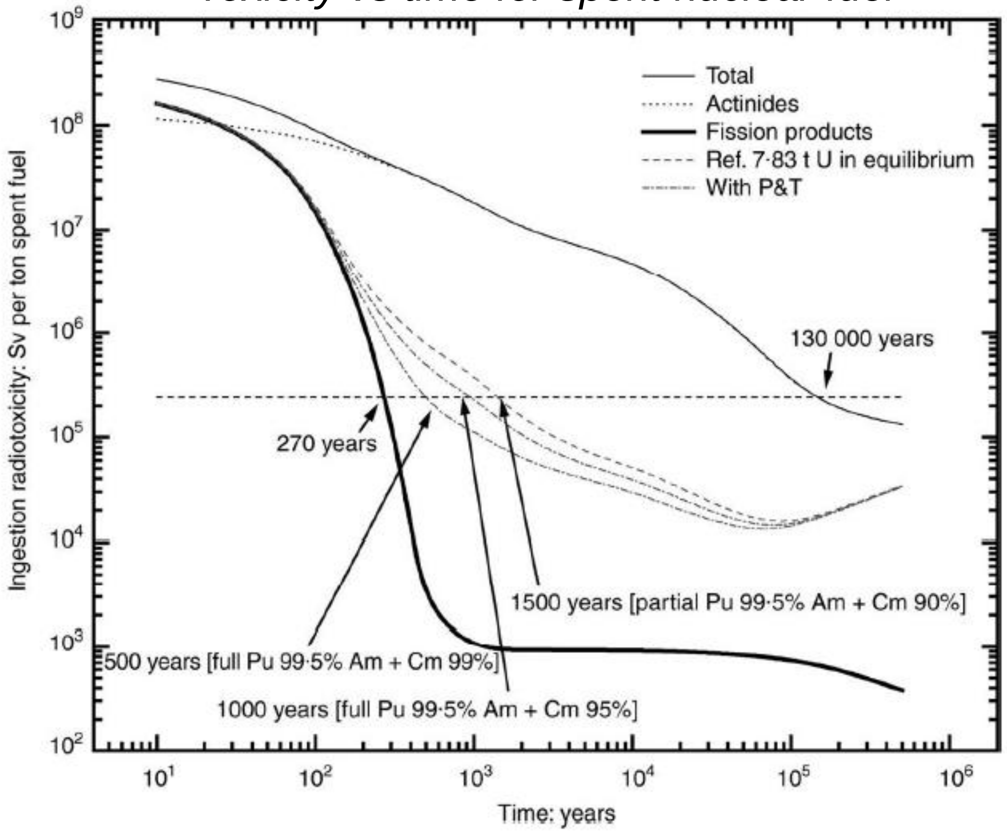

T. Tajima, et al., Fus. Sci. Tech. 77, 251 (2021)

The PULSE division at LLE is a center for innovative science, impactful technology, world-class education, and engaged collaboration

PLASMA & ULTRAFAST LASER SCIENCE & ENGINEERING
UNIVERSITY OF ROCHESTER, LABORATORY FOR LASER ENERGETICS

Dustin Froula (Director)
dfroula@lle.rochester.edu

Laser Plasma Interactions

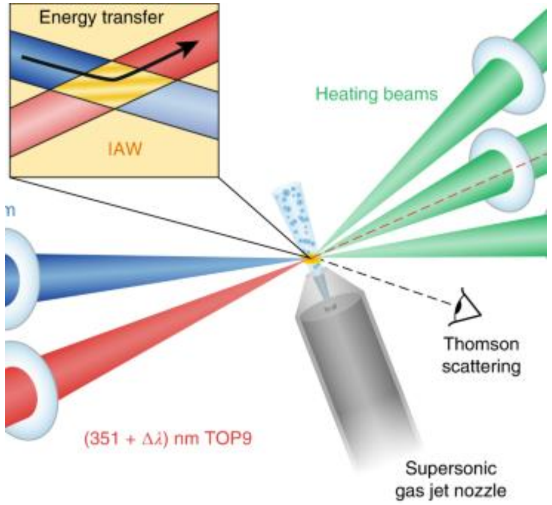

Dave Turnbull (GL)
dpturnbull@lle.rochester.edu

Laser-Plasma Physics

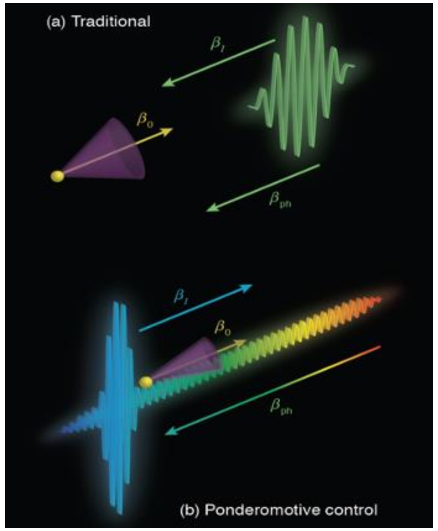

John Palastro (GL)
jpal@lle.rochester.edu

Relativistic Laser-Plasma Experiments

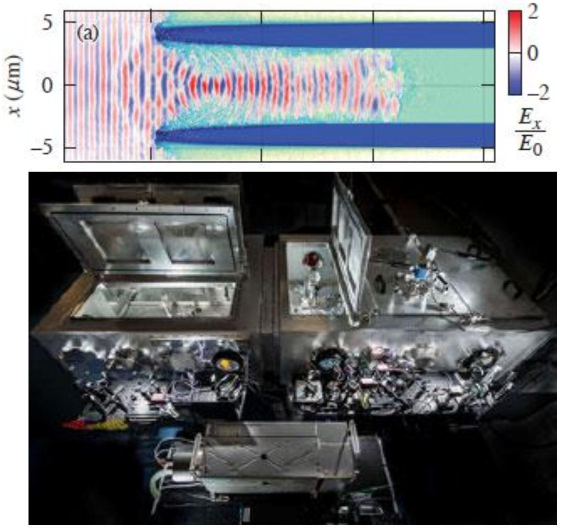

Hans Rinderknecht (GL)
hrin@lle.rochester.edu

Ultrafast Laser-Plasma Diagnostics

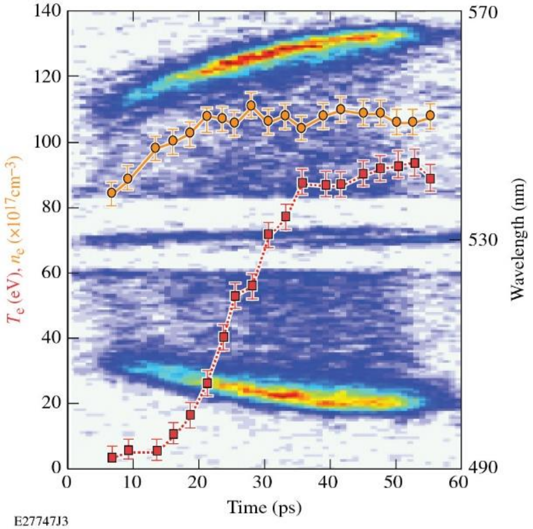

Dustin Froula (acting GL)
dfroula@lle.rochester.edu

Magnetic filaments promise a repeatable and efficient laser-driven source of MT fields, relativistic electrons, and MeV photons

- **Intense lasers in relativistically transparent plasmas generate ultra-strong magnetic fields, trapping and accelerating electrons**
  - Relativistic electrons in ultra-strong B-fields efficiently radiate MeV-scale photons

- **Scaling laws were derived for magnetic filament radiation, and validated with 3-D PIC simulations**
  - Efficiency of >10% is predicted for intensity above 6×10^{21} W/cm^2

- **Experiments on the Texas Petawatt laser have been performed to test these predictions**
  - The predicted electron and photon signatures were observed in a subset of experiments

Appendix A: What about the Alfvén current limit? The current limit is increased for a beam with relativistic velocity.

- **The Alfvén current J_A is the total current a beam of charged particles can carry as limited by self-pinching:**

$$J_A = 4\pi\epsilon_0 \frac{m_e c^3}{|e|}$$

- **For relativistic electrons, this limit is increased with the effective electron mass by the Lorentz factor, γ. The current density for a beam of relativistic electrons with radius R is then:**

$$\pi R^2 j < \gamma J_A$$

- **This condition limits the filament radius:**

$$\frac{R}{\lambda} < \frac{1}{\pi}\sqrt{\frac{\gamma}{\alpha}}$$

- **In this work we assume the electrons are sufficiently relativistic that this condition is fulfilled.**

I. Y. Dodin and N. J. Fisch, Physics of Plasmas 13, 103104 (2006).